Steady state characteristics of a three-phase fluidized bed bioreactor with partial biomass recirculation

Szymon Skoneczny*, Bolesław Tabiś

Cracow University of Technology, Department of Chemical and Process Engineering,
ul. Warszawska 24, 30-155 Kraków, Poland

The paper presents modeling and simulation results of the operation of a three-phase fluidized bed bioreactor with partial recirculation of biomass. The proposed quantitative description of the bioreactor takes into account biomass growth on inert carriers, microorganisms decay and interphase biomass transfer. Stationary characteristics of the bioreactor and local stability of steady-states were determined. The influence of microbiological growth kinetics on the multiplicity of steady-states was discussed. The relationship between biofilm growth and boundaries of fluidized bed existence was shown.

Keywords: fluidized bed, bioreactor, mathematical modeling, steady states

1. INTRODUCTION

Three-phase fluidized bed bioreactors have found numerous applications in environment protection and biotechnology, such as: biodegradation of toxic organic compounds, microbiological nitrification, synthesis of some drugs, e.g. penicillin, oxytetracycline, in the synthesis of some organic compounds and in yeast production. The main advantages of fluidized bed bioreactors include above all: strongly developed interphase surface, increase of overall biomass concentration in the bioreactor and elimination of bed clogging, which is observed in vessels with a stationary bed. Due to the numerous applications of three-phase fluidized-bed bioreactors in biotechnology, studies on mathematical modeling and simulation of these apparatuses have been conducted for many years (Onysko et al., 2002; Park et al., 1984; Tang and Fan, 1987). Previous modeling studies, even relatively new ones, have not taken into account biomass thickening and its recirculation (Olivieri et al., 2011; Onysko et al., 2002; Tang and Fan, 1987; Tang et al., 1987). It is justified to perform steady-state analysis of a fluidized-bed bioreactor equipped with these process solutions which improve the productivity of bioreactors (Kwon et al., 2001). There are also drawbacks of the above-mentioned mathematical models. The distributions of biomass in the biofilm were included only in the study by Tang et al. (1987). On the other hand, the microbiological process in the liquid phase was neglected, which is a far-reaching assumption. The most advanced mathematical model of the three-phase fluidized bed bioreactor was proposed by Olivieri et al. (2011). However, this model does not take into account external resistances of mass transfer between the liquid and the biofilm or decay of microorganisms in the biofilm. In addition, the cited authors did not take into account the distribution of diffusion coefficients in the biofilm or the distribution of its density. Due to the limitations of previously formulated models, in this paper a more general model is proposed, which takes into account: microbiological process proceeding both in liquid phase and in the biofilm, double-substrate growth kinetics, distributions of biomass density and diffusion coefficients in the biofilm, biomass thickening and

---

* Corresponding author, e-mail: skoneczny@chemia.pk.edu.pl

www.czasopisma.pan.pl   PAN   www.journals.pan.pl

S. Skoneczny, B. Tabiś Chem. Process Eng., 2019, 40 (1), 77–86

recirculation, biomass decay in the biofilm, external mass transfer resistances from the gas to the liquid and from the liquid to the biofilm. An analysis was performed of the influence of many important process parameters, which have not yet been addressed in the literature. These parameters are: biomass thickening coefficient, fraction of carrier particles in the liquid, mean residence time of the liquid in the bioreactor and recirculation ratio of the liquid. In order to assess the process properties of the fluidized-bed bioreactor, its steady-state characteristics were compared with those of a classical continuous stirred tank bioreactor without a biofilm.

2. MATHEMATICAL MODEL OF THE BIOREACTOR

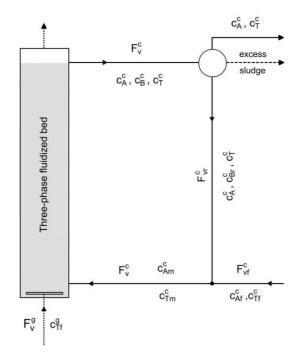The schematic diagram of the analyzed bioreactor is presented in Fig. 1.

Fig. 1. Schematic diagram of the three-phase fluidized bed bioreactor with external recirculation

In a fluidized bed bioreactor microbiological process proceeds in the liquid and biofilm growing on fine particles. Between these both environments there is mass transfer of reactants and biomass. The mathematical model of the bioreactor dynamics is presented in Appendix A. The steady-state form of the model is obtained by equating the derivatives of state variables with respect to time to zero. Therefore, a system of ordinary differential equations and algebraic equations is obtained. Steady state in the biofilm formed on a spherical particle is therefore described by the following differential equations:

$$0 = \frac{d^2\eta}{dz^2} + \left(\frac{1}{D_{eA}(z)}\frac{dD_{eA}(z)}{dz} + \frac{2L_b}{r_0 + L_b z}\right)\frac{d\eta}{dz} - \Phi_A^2 \frac{r_A^b(\eta,\delta,z)}{r_A^c} \tag{1a}$$

$$0 = \frac{d^2\delta}{dz^2} + \left(\frac{1}{D_{eT}(z)}\frac{dD_{eT}(z)}{dz} + \frac{2L_b}{r_0 + L_b z}\right)\frac{d\delta}{dz} - \Phi_T^2 \frac{r_T^b(\eta,\delta,z)}{r_T^c} \tag{1b}$$

where:

$$\Phi_A^2 = \frac{L_b^2 \cdot r_A^c}{D_{eA}(z) \cdot c_A^c} \qquad \text{and} \qquad \Phi_T^2 = \frac{L_b^2 \cdot r_T^c}{D_{eT}(z) \cdot c_T^c} \tag{2}$$

Boundary conditions have the form:

$$\frac{d\eta(0)}{dz} = 0 \tag{3a}$$

$$\frac{d\delta(0)}{dz} = 0 \tag{3b}$$

$$\frac{d\eta(1)}{dz} = \text{Bi}_A \left[1 - \eta(1) \right] \tag{3c}$$

$$\frac{d\delta(1)}{dz} = \text{Bi}_A \left[1 - \delta(1) \right] \tag{3d}$$

where:

$$\text{Bi}_A = \frac{k_{sA} L_b}{D_{eA}(1)} \qquad \text{and} \qquad \text{Bi}_T = \frac{k_{sT} L_b}{D_{eT}(1)} \tag{4}$$

The biofilm thickness at a steady state is calculated using the following formula

$$0 = \frac{1}{3\overline{\rho}_b} \frac{r_b^3 - r_0^3}{r_b^2} \cdot \overline{r}_B^b - \frac{k_{det}}{3} \cdot \frac{r_b^3 - r_0^3}{r_b^2} \tag{5}$$

A process in the liquid phase at steady state conditions can be described by the system of following nonlinear algebraic equations:

$$0 = -\frac{1}{\tau_0^c} \alpha + r_A^c(\alpha, \beta, \gamma) + \frac{a_s}{(1 - \varepsilon_g)(1 - \zeta)} k_{sA}(1 - \alpha)(1 - \eta(1)) \tag{6a}$$

$$0 = \frac{\vartheta\xi - 1}{\tau_0^c(1 - \xi)} \beta + r_B^c(\alpha, \beta, \gamma) + \frac{1}{c_{Af}} \frac{\zeta}{1 - \zeta} \left(\frac{r_b^3}{r_0^3} - 1 \right) \cdot k_{det} x_a \overline{\rho}_b L_b \tag{6b}$$

$$0 = \frac{1}{\tau_0^c}(\gamma_f - \gamma) - r_T^c(\alpha, \beta, \gamma) + \frac{m - K\gamma}{\tau_b(1 - \varepsilon_g)(1 - \zeta)} \left[1 - \exp\left(\frac{-\tau_b a k_{cT}}{K} \right) \right] -$$
$$- \frac{a_s}{(1 - \varepsilon_g)(1 - \zeta)} k_{sT} \gamma (1 - \delta(1)) \tag{6c}$$

where: $m = \dfrac{c_{Tf}^g}{c_{Af}}$, $\tau_b = \dfrac{H_0}{(1 - \varepsilon_g) \cdot u_{0g}}$, $\tau_0^c = \dfrac{V^c}{F_{Vf}^c}$, $x_a = \dfrac{k_{det} L_b}{k_{det} L_b + k_o}$.

Recirculation ratio ξ and the biomass thickening coefficient ϑ are defined as:

$$\xi = \frac{F_{Vr}^c}{F_V^c}, \qquad \vartheta = \frac{c_{Br}}{c_B^c} \tag{7}$$

The form of equations describing the utilization rate of the carbonaceous substrate r_A, oxygen r_T, and biomass growth r_B depends on the microbiological process. For the analysis of microbiological processes two different kinetic models were adopted. The first process is the utilization of glucose by the bacteria *Pseudomonas aeruginosa* following double-substrate Monod-Monod kinetics. Simulations were also performed for the biodegradation of phenol by bacteria *Pseudomonas putida* following double-substrate Haldane-Monod kinetics. Kinetic parameters for these processes are accepted according to works of Seker et al. (1997) and Beyenal et al. (2003).

Dimensionless variables α, β, γ characterizing the liquid phase, dimensionless concentration of carbonaceous substrate in the biofilm, dimensionless concentration of oxygen in the biofilm and the dimensionless coordinate in the biofilm are defined in the following way:

$$\alpha = \frac{c_{Af}^c - c_A^c}{c_{Af}^c}, \qquad \beta = \frac{c_B^c}{c_{Af}^c}, \qquad \gamma = \frac{c_T^c}{c_{Af}^c}, \qquad \eta = \frac{c_A^b}{c_A^c}, \qquad \delta = \frac{c_T^b}{c_T^c}, \qquad z = \frac{x - r_0}{L_b} \tag{8}$$

www.czasopisma.pan.pl   PAN   www.journals.pan.pl

S. Skoneczny, B. Tabiś Chem. Process Eng., 2019, 40 (1), 77–86

3. RESULTS AND DISCUSSION

A comparative analysis of the shape and position of steady-state branches was conducted for aerobic biodegradation of glucose and aerobic biodegradation of phenol. The steady-state analysis covered the assessment of local stability of steady states, according to the method described in Appendix B. Solid lines in figures presented in the further part of the study represent stable steady states, while dashed ones denote unstable steady states.

Figure 2 illustrates steady-state branches with respect to the mean residence time of the liquid, obtained for the biodegradation of glucose for two values of the biomass thickening coefficient ϑ and for two values of the fraction of carrier particles in the liquid ζ.
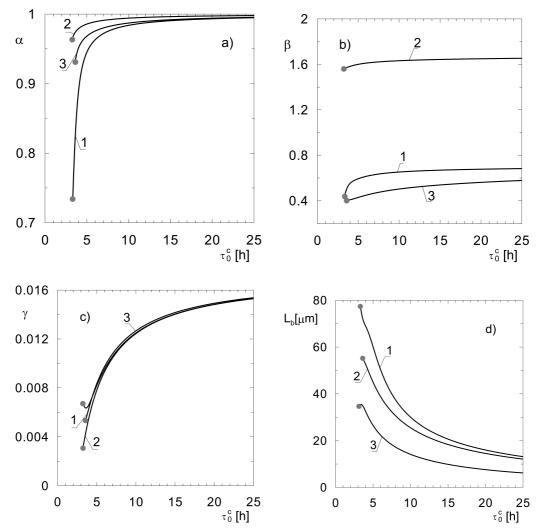

Fig. 2. Steady state branches of three-phase fluidized bed bioreactor for two values of ϑ and two values of ζ (glucose utilization; at grey points the condition $u_{0c} = u_t$ is fulfilled). Lines 1 – $\vartheta = 1.5$ and $\zeta = 0.01$; lines 2 – $\vartheta = 3.5$ and $\zeta = 0.01$; lines 3 – $\vartheta = 1.5$ and $\zeta = 0.05$ ($c_{Af} = 0.5$ kg/m³; $\xi = 0.2$; $\rho_0 = 1400$ kg/m³; $u_{0g} = 0.005$ m/s)

Thickening of biomass and its partial recirculation is used for its retention in the bioreactor. An increase in biomass thickening coefficient increases its concentration in the recirculated stream and therefore biomass concentration in the liquid (Fig. 2b, lines 1 and 2). Hence, the microbiological process rate in the liquid phase increases. As a result, the degree of conversion of the carbonaceous substrate increases (Fig. 2a, lines 1 and 2) which causes a decline in the availability of the carbonaceous substrate for microorganisms in the biofilm. Therefore, the biofilm thickness is reduced (Fig. 2d, lines 1 and 2). Increasing the fraction

of carrier particles in the liquid ζ leads to an increase in the mass transfer surface area between the liquid phase and the biofilm. The result is an increase in the degree of conversion of the carbonaceous substrate (Fig. 2a, lines 1 and 3). On the other hand, the decrease in the concentration of carbonaceous substrate in the liquid phase, associated with increased degree of conversion α reduces the biofilm thickness (Fig. 2d, lines 1 and 3).

Figure 3 illustrates the influence of the mean residence time of the liquid on state variables of the fluidized-bed bioreactor for aerobic biodegradation of phenol. This is a process with inhibiting influence of the carbonaceous substrate. To assess the influence of biomass recirculation and thickening, simulations were performed for two situations, i.e. without recirculation and with the use of biomass recirculation and thickening. Figure 3 additionally shows, for comparison, the steady-state branches obtained for a classical continuous stirred tank bioreactor without a biofilm. It can be seen in Fig. 3 that the phenomenon of steady-state multiplicity is observed associated with substrate inhibition.
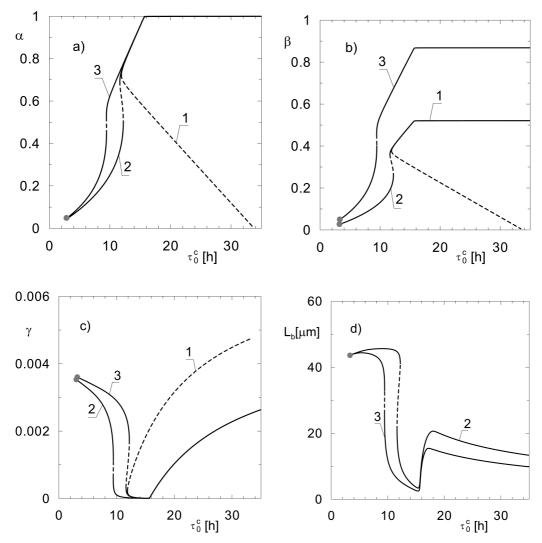

Fig. 3. Comparison of the steady-states branches for tank bioreactor without a biofilm (lines 1) with stationary characteristics of the fluidized-bed bioreactor without recirculation (lines 2) and with partial biomass recirculation and thickening (lines 3 – ξ = 0.5; ϑ = 1.5); solid lines – stable steady states; dashed lines – unstable steady states (phenol biodegradation; at grey points the condition $u_{0c} = u_t$ is fulfilled) (c_{Af} = 1.8 kg/m³; ρ_0 = 2300 kg/m³; u_{0g} = 0.005 m/s)

Fig. 3a shows that for the above mean residence time of about τ_0^c = 12 h the degree of conversion of the carbonaceous substrate is practically the same regardless of the design solution. However, in the case of

www.czasopisma.pan.pl   PAN   www.journals.pan.pl

S. Skoneczny, B. Tabiś Chem. Process Eng., 2019, 40 (1), 77–86

a bioreactor without biofilm there is a risk of biomass wash-out from the apparatus and the loss of its productivity below so-called critical residence time of the liquid (Fig. 3b, line 1). The value of the critical mean residence time corresponds to the turning point on the branch $\beta(\tau_0^c)$. In the case of the fluidized-bed bioreactor (lines 2) below the critical residence time of the liquid, the productivity are maintained, although the degree of conversion drops significantly, which is caused by the increase in the carbonaceous substrate load. The use of biomass recirculation and thickening (lines 3) additionally shifts the turning point towards lower values of the mean residence time of the liquid, and moreover, a greater degree of conversion of toxic carbonaceous compound is obtained. According to the expectation, biomass recirculation increases the suspended biomass concentration (Fig. 3b, line 3). Following the increase in the microbiological process rate in the liquid, the availability of the carbonaceous substrate for attached bacteria is limited and therefore the biofilm thickness decrease. For these reasons, the use of this design solution is justified. The steady-state branches can be used also to determine the conditions of the bioreactor aeration. The results indicate insufficient aeration of the reactor, as evidenced by the dissolved oxygen concentration close to zero (Fig. 3c) for mean residence time of the liquid in the range 12 h $<$ τ_0^c $<$ 16 h. The anoxia of the reaction environment results in reduced degree of conversion α, biomass concentration β and the biofilm thickness L_b in this range of τ_0^c. From the comparison of steady-state branches $\gamma(\tau_0^c)$ obtained for phenol degradation (Fig. 3c) and that of glucose utilization (Fig. 2c) it can be seen that in the latter process, there is no region of oxygen depletion. It happens for two reasons. Steady-state branches presented in Fig. 2 were obtained for significantly lower carbonaceous substrate concentration in the feed stream than for those presented in Fig. 3. Lower carbonaceous substrate load is related to a lower oxygen requirement for the microbiological process. The second reason is that in phenol degradation a larger amount of oxygen is used per mass of carbonaceous substrate utilized by bacteria, which is expressed by the yield coefficient w_{TA}. For phenol degradation this coefficient is equal w_{TA} = 1.541 (Seker et al., 1997), while for glucose utilization it is w_{TA} = 0.989 (Beyenal et al., 2003).

4. CONCLUSIONS

The paper presents a mathematical model of a three-phase fluidized bed bioreactor which takes into account biomass thickening and recirculation. steady-state characteristics of the bioreactor for two microbiological processes were presented. it was shown that multiple steady states appear in the process with substrate inhibition.

The obtained steady-state branches prove that the use of partial biomass recirculation and thickening is justified, because it improves process safety and increases bioreactor productivity. Increasing the fraction of carrier particles in the liquid ζ also increases the efficiency of the bioreactor.

SYMBOLS

a_s	specific external biofilm surface area, m^{-1}
ak_c	gas-liquid volumetric mass transfer coefficient, h^{-1}
Bi_i	Biot number, (i = A, T), –
c_A, c_B, c_T	mass concentration of carbonaceous substrate, biomass and oxygen, respectively, kg·m^{-3}
d_0	diameter of a solid carrier, m
D_e	effective diffusion coefficient in biofilm, m^2·h^{-1}
F_V	volumetric flow rate, m^3·h^{-1}
H_0	height of the liquid phase without gas bubbles, m
K	gas-liquid interphase equilibrium constant, –

k_{det}	biofilm detachment rate coefficient, $\text{m}^{-1} \cdot \text{h}^{-1}$
k_s	liquid-biofilm mass transfer coefficient, $\text{m} \cdot \text{h}^{-1}$
L_b	thickness of the biofilm, m
r_A, r_T	uptake rate of carbonaceous substrate and oxygen, respectively, $\text{kg} \cdot \text{m}^{-3} \cdot \text{h}^{-1}$
r_B	growth rate of biomass, $\text{kg} \cdot \text{m}^{-3} \cdot \text{h}^{-1}$
$\overline{r}_B^b$	average biomass growth rate in the biofilm, $\text{kg} \cdot \text{m}^{-3} \cdot \text{h}^{-1}$
r_b	radius of the bioparticle, m
r_{det}	detachment rate of biomass, $\text{kg} \cdot \text{m}^{-3} \cdot \text{h}^{-1}$
r_0	radius of the carrier particle, m
u	superficial velocity, $\text{m} \cdot \text{s}^{-1}$
u_b	bubble rise velocity, $\text{m} \cdot \text{s}^{-1}$
u_t	terminal velocity of bioparticles, $\text{m} \cdot \text{s}^{-1}$
u_{0g}	superficial air velocity, $\text{m} \cdot \text{s}^{-1}$
w_{TA}	yield coefficient of oxygen with regard to the carbonaceous substrate, $(\text{kg T}) \cdot (\text{kg A})^{-1}$
V	volume, m^3
x_a	fraction of active biomass in the biofilm,–
z	dimensionless coordinate in the biofilm, –
α	degree of conversion of the carbonaceous substrate, –
β	dimensionless concentration of biomass in liquid phase, –
γ	dimensionless concentration of oxygen in liquid phase, –
δ	dimensionless concentration of oxygen in the biofilm, –
ε_g	gas hold-up in the multi-phase system, –
ζ	fraction of carrier particles in the liquid, –
η	dimensionless concentration of carbonaceous substrate in the biofilm, –
ϑ	biomass thickening coefficient, –
ξ	recirculation ratio of the liquid, –
ρ_b	concentration of biomass in the biofilm, $\text{kg} \cdot \text{m}^{-3}$
$\overline{\rho}_b$	average concentration of biomass in the biofilm, $\text{kg} \cdot \text{m}^{-3}$
ρ_0	density of solid carrier, $\text{kg} \cdot \text{m}^{-3}$
τ_0^c	mean residence time of the liquid in the installation, h
Φ	Thiele modulus, –

Superscripts

b	biofilm phase
c	liquid (continuous) phase
g	gas phase

Subscripts

A, B, T	refers to carbonaceous substrate, biomass and oxygen, respectively
s	refers to surface of the biofilm
f	refers to feed stream
r	refers to recirculated stream

REFERENCES

Beyenal H., Chen S.N., Lewandowski Z., 2003. The double substrate growth kinetics of Pseudomonas aeruginosa. *Enzyme Microb. Technol.*, 32, 92–98. DOI: 10.1016/S0141-0229(02)00246-6.

Kwon S., Yoo I-K, Lee W.G., Chang H.N., Chang Y.K. 2001. High-rate continuous production of lactic acid by *Lactobacillus rhamnosus* in a two-stage membrane cell-recycle bioreactor. *Biotechnol Bioeng.*, 73, 25–34. DOI: 10.1002/1097-0290(20010405)73:1<25::AID-BIT1033>3.0.CO;2-N.

www.czasopisma.pan.pl   PAN   www.journals.pan.pl

S. Skoneczny, B. Tabiś Chem. Process Eng., 2019, 40 (1), 77–86

Olivieri G., Russo M.E., Marzocchella A., Salatino P., 2011. Modeling of an aerobic biofilm reactor with double-limiting substrate kinetics: Bifurcational and dynamical analysis. *Biotechnol. Prog.*, 27, 1599–1613. DOI: 10.1002/btpr.690.

Onysko K.A., Robinson C.W., Budman H.M., 2002. Improved modelling of the unsteady-state behaviour of an immobilized-cell, fluidized-bed bioreactor for phenol biodegradation. *Can. J. Chem. Eng.*, 80, 239–252. DOI: 10.1002/cjce.5450800209.

Park Y., Davis M.E., Wallis D.A., 1984. Analysis of a continuous, aerobic, fixed-film bioreactor. II. Dynamic behavior. *Biotechnol. Bioeng.*, 26, 468–476. DOI: 10.1002/bit.260260510.

Seker S., Beyenal H., Salih B., Tanyolac A., 1997. Multi-substrate growth kinetics of *Pseudomonas putida* for phenol removal. *Appl. Microbiol. Biotechnol.*, 47, 610–614. DOI: 10.1007/s002530050982.

Seydel R., 2009. Practical bifurcation and stability analysis. 3rd edition, Springer, New York. DOI: 10.1007/978-1-4419-1740-9.

Tang W., Fan L., 1987. Steady state phenol degradation in a draft-tube, gas-liquid-solid fluidized-bed bioreactor. *AIChE J.*, 33, 239–249. DOI: 10.1002/aic.690330210.

Tang W., Wisecarver K., Fan L., 1987. Dynamics of a draft tube gas-liquid-solid fluidized bed bioreactor for phenol degradation. *Chem. Eng. Sci.*, 42, 2123–2134. DOI: 10.1016/0009-2509(87)85033-9.

APPENDIX A

Mathematical model of the bioreactor dynamics

The dynamics of the microbiological process in the biofilm can be described by the following system of equations:

$$\frac{\partial \eta}{\partial t} = \frac{\eta}{1-\alpha}\frac{d\alpha}{dt} + \frac{D_{eA}(z)}{L_b^2}\left[\frac{\partial^2 \eta}{\partial z^2} + \left(\frac{1}{D_{eA}(z)}\frac{dD_{eA}(z)}{dz} + \frac{L_b z}{D_{eA}(z)}\frac{dL_b}{dt} + \frac{2L_b}{r_0 + L_b z}\right)\frac{\partial \eta}{\partial z}\right.$$
$$\left. -\Phi_A^2 \frac{r_A^b(\eta, \delta, z)}{r_A^c}\right] \tag{A1a}$$

$$\frac{\partial \delta}{\partial t} = -\frac{\delta}{\gamma}\frac{d\gamma}{dt} + \frac{D_{eT}(z)}{L_b^2}\left[\frac{\partial^2 \delta}{\partial z^2} + \left(\frac{1}{D_{eT}(z)}\frac{dD_{eT}(z)}{dz} + \frac{zL_b}{D_{eT}(z)}\cdot\frac{dL_b}{dt} + \frac{2L_b}{r_0 + L_b z}\right)\frac{\partial \delta}{\partial z}\right.$$
$$\left. -\Phi_T^2 \frac{r_T^b(\eta, \delta, z)}{r_T^c}\right] \tag{A1b}$$

$$\frac{dL_b}{dt} = \frac{L_b}{\overline{\rho}_b(r_0 + L_b)^2}\int_0^1 (r_0 + zL_b)^2 \cdot r_B^b(z)dz - \frac{k_{det}}{3(r_0 + L_b)^2}\left[(r_0 + L_b)^3 - r_0^3\right] \tag{A1c}$$

Initial and boundary conditions related to Eqs. (A1) are:

$$\eta(z, 0) = \eta_0(z) \tag{A2a}$$

$$\delta(z, 0) = \delta_0(z) \tag{A2b}$$

$$L_b(0) = L_{b0} \tag{A2c}$$

$$\frac{\partial \eta(0, t)}{\partial z} = 0 \tag{A3a}$$

$$\frac{\partial \delta(0, t)}{\partial z} = 0 \tag{A3b}$$

$$\frac{\partial \eta(1, t)}{\partial z} = \text{Bi}_A \left[1 - \eta(1, t) \right] \tag{A3c}$$

$$\frac{\partial \delta(1, t)}{\partial z} = \text{Bi}_T \left[1 - \delta(1, t) \right] \tag{A3d}$$

where: $\text{Bi}_A = \dfrac{k_{sA} L_b}{D_{eA}(1)}$ and $\text{Bi}_T = \dfrac{k_{sT} L_b}{D_{eT}(1)}$.

The dynamics of the biofilm thickness has a form:

$$\frac{dL_b}{dt} = \frac{1}{3\overline{\rho}_b} \frac{r_b^3 - r_0^3}{r_b^2} \cdot \overline{r}_B^b - \frac{k_{det}}{3} \cdot \frac{r_b^3 - r_0^3}{r_b^2} \tag{A4}$$

with initial condition:

$$L_b(0) = L_{0b} \tag{A5}$$

Dimensionless form of equations describing the dynamics of the liquid phase can be presented as:

$$\frac{d\alpha}{dt} = -\frac{1}{\tau_0^c} \alpha + r_A^c(\alpha, \beta, \gamma) + \frac{a_s}{(1 - \varepsilon_g)(1 - \zeta)} k_{sA}(1 - \alpha)(1 - \eta(1, t)) \tag{A6a}$$

$$\frac{d\beta}{dt} = \frac{\vartheta \xi - 1}{\tau_0^c(1 - \xi)} \beta + r_B^c(\alpha, \beta, \gamma) + \frac{1}{c_{Af}} \frac{\zeta}{1 - \zeta} \left(\frac{r_b^3}{r_0^3} - 1 \right) \cdot k_{det} x_a \overline{\rho}_b \tag{A6b}$$

$$\frac{d\gamma}{dt} = \frac{1}{\tau_0^c} \left(\gamma_f - \gamma \right) - r_T^c(\alpha, \beta, \gamma) + \frac{m - K\gamma}{\tau_b(1 - \varepsilon_g)(1 - \zeta)} \left[1 - \exp \left(\frac{-\tau_b a k_{cT}}{K} \right) \right]$$
$$- \frac{a_s}{(1 - \varepsilon_g)(1 - \zeta)} k_{sT} \gamma \left(1 - \delta(t, 1) \right) \tag{A6c}$$

where $m = \dfrac{c_{Tf}^g}{c_{Af}}$, $\tau_b = \dfrac{H_0}{(1 - \varepsilon_g) \cdot u_{0g}}$, $\tau_0^c = \dfrac{V^c}{F_{Vf}^c}$.

Eqs. (A6) are accompanied by the following initial conditions

$$\alpha(0) = \alpha_0, \qquad \beta(0) = \beta_0, \qquad \gamma(0) = \gamma_0 \tag{A7}$$

APPENDIX B

Assessment of local stability of steady states

The boundary value problem describing the process in the biofilm, i.e. Eqs. (1) and (3), was transformed using orthogonal collocation method to a system of nonlinear algebraic equations:

$$\sum_{i=1}^{N=1} g_{ji} \eta_i + \left(\frac{1}{D_{eA}(z_j)} \frac{dD_{eA}(z_j)}{dz} + \frac{2L_b}{r_0 + L_b z} \right) \cdot \sum_{i=1}^{N=1} m_{ji} \eta_i - \Phi_A^2 \frac{r_A^b(\eta_j, \delta_j, z_j)}{r_A^c} = 0 \tag{B1a}$$

$$\sum_{i=1}^{N=1} g_{ji} \delta_i + \left(\frac{1}{D_{eT}(z_j)} \frac{dD_{eT}(z_j)}{dz} + \frac{2L_b}{r_0 + L_b z} \right) \cdot \sum_{i=1}^{N=1} m_{ji} \delta_i - \Phi_T^2 \frac{r_T^b(\eta_j, \delta_j, z_j)}{r_T^c} = 0 \tag{B1b}$$

www.czasopisma.pan.pl   PAN   www.journals.pan.pl

S. Skoneczny, B. Tabiś Chem. Process Eng., 2019, 40 (1), 77–86

$$\sum_{i=1}^{N=1} m_{(N+1)i}\eta_i + \mathrm{Bi_A}(1 - \eta_{N+1}) = 0 \qquad \text{(B1c)}$$

$$\sum_{i=1}^{N=1} m_{(N+1)i}\delta_i + \mathrm{Bi_T}(1 - \eta_{N+1}) = 0 \qquad \text{(B1d)}$$

Subscript j in Eqs. (B1a) and (B1b) changes from 1 to N, where N is a number of interior collocation points. Coefficients g_{ji} and m_{ji} are elements of matrices $\boldsymbol{M}$ and $\boldsymbol{G}$, where

$$\boldsymbol{M} = \boldsymbol{C} \cdot \boldsymbol{Q}^{-1}, \qquad \boldsymbol{G} = \boldsymbol{D} \cdot \boldsymbol{Q}^{-1} \qquad \text{(B2)}$$

where $\boldsymbol{Q}$ is the matrix of approximating polynomials in collocation points, $\boldsymbol{C}$ is the matrix of first-order derivatives of these polynomials and $\boldsymbol{D}$ is the matrix of second-order derivatives of these polynomials. Legendre orthogonal polynomials of even orders were applied.

The system of Eqs. (B2) is completed with Eqs. (6) for the liquid phase and Eq. (5), which determines biofilm thickness. For the assessment of steady-state stability it is sufficient to determine eigenvalues of Jacobi matrix of right-hand sides of the nonlinear algebraic equations obtained in this way (Seydel, 2009).